INL/CON-23-71179-Revision-0

FINITE ELEMENT MODEL MESH REFINEMENT EFFECTS ON QUALIFICATION OF NUCLEAR GRADE GRAPHITE COMPONENTS

Changing the World's Energy Future

Andrea L Mack, William E Windes, Joseph Bass, William M Hoffman

INL/CON-23-71179-Revision-0

FINITE ELEMENT MODEL MESH REFINEMENT EFFECTS ON QUALIFICATION OF NUCLEAR GRADE GRAPHITE COMPONENTS

Andrea L Mack, William E Windes, Joseph Bass, William M Hoffman

July 2023

Idaho National Laboratory
Idaho Falls, Idaho 83415

http://www.inl.gov

Prepared for the
U.S. Department of Energy
Under DOE Idaho Operations Office
Contract DE-AC07-05ID14517

Proceedings of the ASME 2023
Pressure Vessels & Piping Conference
PVP2023
July 16-21, 2023, Atlanta, Georgia, USA

PVP2023-107369

FINITE ELEMENT MODEL MESH REFINEMENT EFFECTS ON QUALIFICATION OF NUCLEAR GRADE GRAPHITE COMPONENTS

Andrea Mack[1], William Hoffman[1], Joseph Bass[1], William Windes[1]

[1]Idaho National Laboratory, Idaho Falls, ID

ABSTRACT

The American Society of Mechanical Engineers (ASME) provides the full and simplified design-by-analysis probabilistic assessments for determining acceptance of nuclear grade graphite core components. The assessments can be characterized by three parts: (1) a component stress distribution, often determined by a finite element (FE) model; (2) a Weibull probability density function (pdf) that characterizes the experimental tensile strength distribution; and (3) the post-processor, which combines the FE model and the Weibull strength distribution in accordance with the full and simplified assessments to determine component acceptance. It is known that the level of mesh refinement in FE models can affect the modeled component's calculated stress distribution. Depending on the component geometry, the stress distribution may converge with sufficient refinement. It was previously unknown whether the acceptance decision resulting from the full and simplified assessments might change even with sufficient mesh refinement. This study explores that question using experimental strength results for a dog-bone geometry for two graphite grades, IG-110 and PCEA. The simplified assessment has two criteria that must be met, the first limits the combined membrane stress by the allowable stress and the second limits the peak equivalent stress by the allowable stress scaled by the ratio of flexural to tensile strength. In the application of the simplified assessment, convergence of the peak equivalent stress required extreme mesh refinement, however, the acceptance decision was not affected. It is hypothesized that more complex geometries with stress concentrations may present mesh refinement effects on the simplified assessment acceptance decision. Mesh refinement did affect the acceptance decision in the full assessment for the applied pressure loadings in this study. This work suggests component stress distribution convergence is not a sufficient criteria for POF convergence in the full assessment and that mesh refinement should continue until the POF has converged, especially where the resulting POF is bordering the SRC acceptable POF limit.

Keywords: ASME, full assessment, simplified assessment, qualification, nuclear, graphite, Weibull, probability, failure, finite element analysis, convergence, strength, stress

NOMENCLATURE

α	3-parameter Weibull shape parameter
β	3-parameter Weibull scale parameter
μ	3-parameter Weibull threshold parameter
V_m	minimum link volume
Δ	relative stress range parameter
R_{tf}	ratio of the flexural mean strength to the tensile mean strength
C_m	combined membrane stress
ASME	American Society of Mechanical Engineers
BPVC	Boiler and Pressure Vessel Code
FE	Finite Element
LB	Lower Bound
MLE	Maximum Likelihood Estimate
POF	Probability of Failure
POS	Probability of Survival
SRC	Structural Reliability Class
pdf	probability density function
cdf	cumulative density function

1. INTRODUCTION

The next generation of nuclear reactors include High Temperature and Very High Temperature Reactor (HTR and VHTR) designs [6]. These advanced reactor designs utilize thermally stable graphite as core internal components [7] using an inert coolant, composed of either gas or molten salt. The American Society of Mechanical Engineers (ASME) Boiler and Pressure Vessel Code (BPVC) Section III, Division 5 specifies Rules for Construction of Nuclear Facility Components for High Temperature Reactors [3]. Subsection HH Subpart A, Article 3000 (HHA-3000) provides design guidelines for class SN nonmetallic core components, specifically graphite components.

Graphite is a quasi-brittle material with inherent pore and flaw distributions [8,9]. Thus, HHA-3000 implements probabilistic methods to set acceptance limits through two design-by-analysis alternatives for qualification, the simplified and full assessments. The simplified assessment uses a 2-parameter Weibull distribution to describe the tensile strength distribution of the given graphite grade to determine an allowable stress. Two requirements must be met to satisfy the simplified assessment, one based on the component's combined membrane stress (C_m) and one based on the component's peak equivalent stress, often found using finite element (FE) analysis. The full assessment uses a 3-parameter Weibull distribution and groups the elements throughout the component based on the magnitude of the equivalent stress. The output is a component probability of failure (POF), which is compared to a POF limit. Design-by-test is a third alternative but is not discussed in this paper.

IG-110 and PCEA graphite grades with the dog-bone mechanical test geometry were used in this study to investigate the effect of mesh refinement on the simplified and full assessments. This paper explains the full and simplified assessment methodologies and applies those methods to dog-bone tensile test data fabricated from current nuclear graphite grades IG-110 and PCEA. Finite element modeling is performed with five mesh refinements. The full assessment implements a step that groups mesh elements. The grouping criteria changed between the 2019 and 2021 Code versions, therefore this study is applied based on both Code versions. Results and implications of mesh refinement on component acceptance per HHA-3000 is discussed, as well as other considerations.

1.1 Background

Neither the full nor simplified graphite component assessments of the ASME BPVC [3] specify FE modeling mesh refinement guidelines. It is common practice in FE modeling to continue mesh refinement until stress distribution convergence has been obtained. While a designer might demonstrate stress convergence in their application, the question was opened as to whether stress convergence corresponds to: (1) convergence in the peak equivalent stress used in the simplified assessment (HHA-II-3300); and (2) convergence in the POF found using the methodology specified within the full assessment, sub-article HHA-3217. Since no mesh refinement guidelines are provided, it is necessary to understand whether refinement beyond a typical converged stress distribution is necessary to achieve consistent acceptance decisions.

1.2 Related Work

Hindley performed much of the foundational work for the full assessment implemented in HHA-3217. In his paper [4], he discusses having done some mesh refinement studies on POF convergence. In most cases, it appears Hindley used two or three mesh refinements. Hindley claims POF convergence is met before mesh convergence in most cases [4], but details are not explained. The studies in [4] only represent results for NBG-18 and the 2019 Code version.

2. MATERIALS AND METHODS

2.1 ASME BPVC HHA Methods

There are five loading groups for which acceptance limits are applied: Design and Service Levels A, B, C, and D. The limits for each of the loading groups are dependent on the structural reliability class (SRC) of the component. This work is limited to safety class components, SRC-1, which are associated with a POF limit of 10^{-4} and Design and Service Levels A, B and C. Figure HHA-3221-1 in the ASME Code [3] outlines the criteria for graphite core component acceptance.

The assessments can be characterized by three parts: (1) a FE model of the component; (2) a Weibull probability density function (pdf) that characterizes the experimental tensile strength distribution; and (3) the post-processor, which combines the FE model and the Weibull strength distribution in accordance with the full and simplified assessments to determine component acceptance. The simplified and full assessments are briefly described in the following subsections for immediate reference.

2.1.1 Weibull Distribution

Both full and simplified assessments require experimental tensile strength data and component FE equivalent tensile stresses as inputs. Both full and simplified assessments make use of the Weibull pdf, denoted $f(x)$, to characterize the grade's random tensile strength distribution. The pdf maps strengths to probabilities associated with failure. The cumulative density function (cdf) is the integral of a pdf, and as its name implies, it provides the probability of failing at or below a given strength. The 3-parameter Weibull cdf is defined by the shape (α), scale (β) and threshold (μ) parameters. Notation choice corresponds to that found in HHA-II-3200 of [3]. The 3-parameter Weibull cdf is given below.

$$F(x|\alpha,\beta,\mu) = 1 - e^{-\left(\frac{x-\mu}{\beta}\right)^{\alpha}} \quad (1)$$

The Code utilizes one-sided 95% lower bounds for the shape and scale parameters. New notation is not introduced for lower bounds in this paper. When the notation is representative of lower bounds, it is indicated in text.

2.1.2 Simplified Assessment

The simplified assessment is primarily laid out in sections HHA-II-3100 and HHA-II-3300 and Figure HHA-II-3221-1 in [3]. It uses the 2-parameter Weibull distribution, which is found by setting the threshold parameter to 0 in Equation 1. This makes strengths close to 0 have a non-zero probability of failure, though still quite small. $F(x|\alpha,\beta,\mu)$ is set to the SRC-1 POF limit, $F(x|\alpha,\beta,\mu) = 10^{-4}$. Equation 1 is then inverted to solve for the stress associated with the SRC POF limit [denoted $S_g(10^{-4})$], as shown in Equation 2. Equation 2 corresponds to Eq. 21 in HHA-II-3300 [3], with different notation. The 95% one-sided confidence interval lower bounds are obtained for the shape and scale parameters and used in place of β and α to add conservatism to the distribution prior to the calculation of $S_g(10^{-4})$.

$$S_g(10^{-4}) = \beta(-\ln(1-10^{-4}))^{\frac{1}{\alpha}} \quad (2)$$

$S_g(10^{-4})$ is multiplied by the ratio of the flexural mean strength to the tensile mean strength (R_{tf}) to arrive at the allowable stress value.

The equivalent stress in the component can be computed using the equation outlined in HHA-3213. This formulation is derived from the maximum strain energy failure theory. The peak equivalent stress value is computed in the component FE model, then compared to the allowable stress value.

Two criteria must be met to satisfy the simplified assessment:

- $C_m < S_g(10^{-4})$
- $Peak\ equivalent\ stress < R_{tf} * S_g(10^{-4})$

If both criteria are met, the component is accepted per the simplified assessment.

2.1.3 Full Assessment

The full assessment is primarily outlined in HHA-3217 and HHA-II-3200. It summarizes the experimental tensile strength data using the 3-parameter Weibull distribution given in Equation 1. A shortened version of the steps are as follows:

- The threshold parameter is reduced if the component stress distribution and Weibull strength distribution have too little overlap
- The FE integration points are grouped based on:
    - A minimum link (group) volume requirement, V_m
    - A minimum relative (group) stress range, Δ
- A probability of survival (1 – probability of failure) is computed for each group
- The product of the group survival probability (POS) is calculated
- The POF is found as 1-POS and compared to 10^{-4}
- If POF<10^{-4}, the component is accepted

HHA-3217 [3] and [5] give more detailed explanations, which are needed for accurate implementation.

2.2 Code Assessment Assumptions

This study set out to apply the Code rules as they are written in the 2019 and 2021 Code versions. Work presented at the SMiRT conference in 2015 [10] showed that not updating the shape parameter when the threshold is reduced in the full assessment led to erroneous results. Therefore, the shape parameter was updated in the full assessment in this study when the threshold was reduced, though this is not currently specified in the Code.

Points that did not meet grouping criteria at the end of the equivalent stress list were discarded under the assumptions that: (1) these points have the lowest stresses and will not contribute notably to the POF; and (2) the grouping criterion need to be met for the groups to be valid. The Code does not discuss how to deal with this.

The analyses performed were done to represent the 2019 and 2021 Code versions as written, conditional on the assumptions presented here.

2.3 Finite Element Modeling

2.3.1 Methodology

For both the simplified and full assessments, FE models were created and analyzed to obtain the required equivalent tensile stress outputs. A tensile "dog-bone" geometry was used in this mesh refinement study. The finite element modeling tool, Grizzly [1], was developed at Idaho National Laboratory (INL) and was used to compute the necessary stress output for the component. Grizzly is based on the open-source finite element modeling framework, MOOSE [2], also developed at INL. Efforts are currently underway to implement the full and simplified assessment methods into the Grizzly code as a post-processor.

2.3.2 Assumptions

The FE geometry was selected to match the experimental testing done in the Baseline Unirradiated Graphite Program. In order to reduce compute times, the model was simplified to a half symmetry bar, cut on the plane intersecting the center perpendicular to the axis of rotation. The grooves on each end, as shown in the drawing, are used in the mechanical test to grip the specimen and apply the axial load. In the model, the loading was applied using a pressure boundary condition, and the material at and above those notches was excluded. A red box is shown in the drawing to illustrate the portion of the specimen used in the model. Figure 1 below shows the drawings for the tensile bar and the resulting FE model.

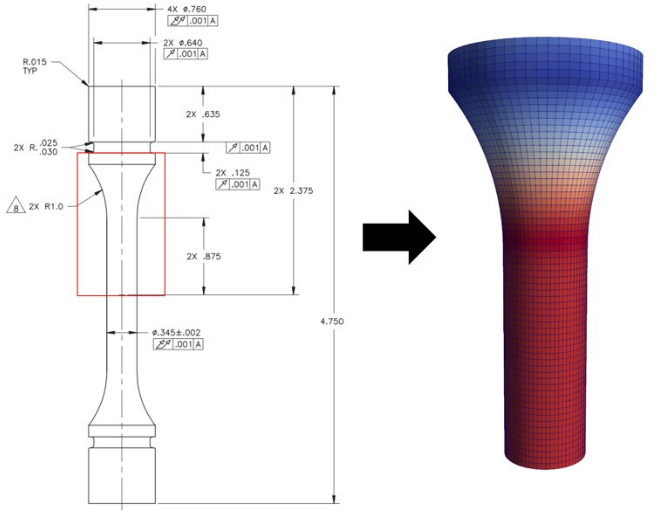

Figure 1: DRAWING FOR TENSILE "DOG-BONE" SPECIMEN. THE RED BOX OUTLINES THE SECTION OF THE COMPONENT USED IN THE FE MODEL, WHICH IS SHOWN TO THE RIGHT. DRAWING DIMENSIONS ARE SHOWN IN INCHES, ALTHOUGH ALL ANALYSES USED METRIC UNITS.

The diameters at the large and small ends are 19.3 and 8.76 mm, respectively. The length of the model shown is 41.02 mm, the length of the small diameter portion is 22.225 mm and the radius of curvature on the fillet is 25.4 mm.

Two nodes on the large surface were constrained to fix translation and rotational modes. Zero axial displacement was applied at the small surface for symmetry, and a uniform pressure load was applied at the large surface in order to axially load the specimen in tension.

2.4 Mesh Refinement Study

An important aspect of FE modeling that must be considered is the effect of mesh size on the solution. In general, smaller elements will provide a more accurate solution; however, models with a significant number of elements can quickly become very expensive in terms of computational costs. The analyst is therefore required to consider costs vs. benefits when selecting a mesh for his or her model, where computational requirements are weighed against model resolution.

In order to address this issue, it is common practice for the analyst to conduct a mesh convergence study. In such a study, sequential meshes are created where each model contains smaller elements than the last. All of the meshes are then analyzed with identical parameters and conditions. The solutions from the various meshes are compared to identify the element size at which further refinement has little effect on the results. It is then up to the modeler to select the appropriate element size for use in the analysis using the mesh convergence study to justify that decision.

The dog-bone tensile component was selected for this analysis because the Weibull strength distribution used in the full and simplified assessments is a tensile strength distribution. While the assessments are used with a variety of geometries, they should be most accurate for the dog-bone geometry.

In order to consider mesh effects, multiple element sizes were considered. Five total meshes were created in order to evaluate the mesh refinement effects on component acceptance. The coarsest mesh was created with an average element length of 0.2 inches. That value was cut in half for each of the subsequent meshes created, such that the final mesh contained elements with an average length of 0.0125 inches. Figure 2 below shows the five meshes used in the analysis.

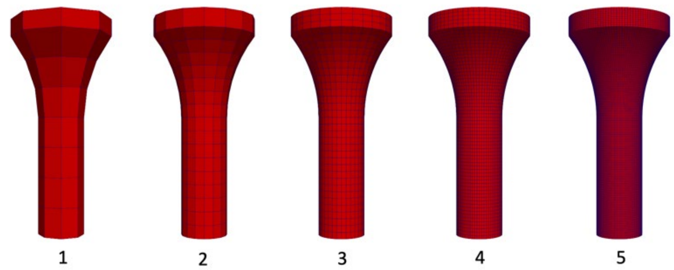

Figure 2: FIVE MESHES USED IN MESH CONVERGENCE STUDY FOR THE DOG-BONE TENSILE SPECIMEN.

In order to evaluate the convergence of stress with mesh refinement in the component, the equivalent stress was measured along the center axis of the model using average element average values. The equivalent stress formula is defined in HHA-3213 of [3]. The stress along the line for each model was plotted in Figure 3.

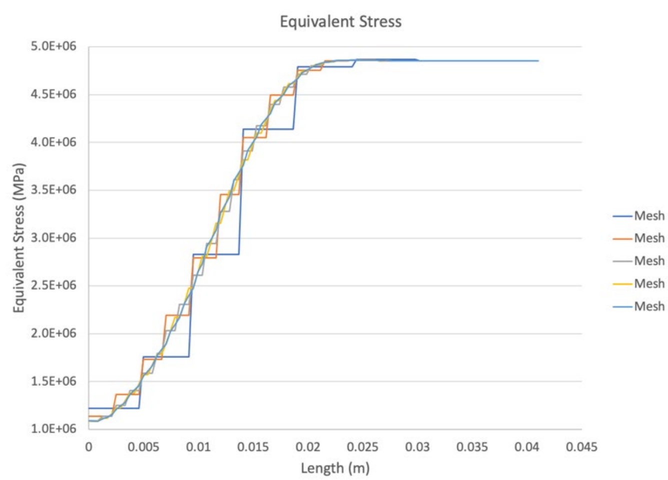

Figure 3: PLOT OF EQUIVALENT STRESSES USING ELEMENT AVERAGE VALUES THROUGH THE CENTER OF THE MODEL.

With a load of 1 MPa applied to the top surface, the analytical solution in the gauge region is 4.853 MPa. All meshes resulted in a stress at the end surface of 4.853 MPa, but the increased mesh refinement models provided higher resolution in the portion of the model where the cross-sectional area changes.

2.5 Data

2.5.1 Experimental Strength Data

Experimental strength data were used from the Unirradiated Graphite Testing Baseline Program for two graphite grades of IG-110 and PCEA tensile test dog-bone specimens. A total of 290 IG-110 specimens from two billets and a total of 127 PCEA specimens from a single billet (billet 01D336, referred to as PCEA36), were used to determine the corresponding Weibull strength distributions. Table 1 displays the Weibull lower bound distributions used in this analysis for each grade.

Table 1: WEIBULL PARAMETER ESTIMATES

	Assessment	μ	α	β
Grade			Lower Bound	Lower Bound
IG-110	Simplified	0	14.804	27.515
	Full	15.129	6.2645	12.292
PCEA36	Simplified	0	5.7433	19.273
	Full	9.9526	2.4870	8.947

Figures 4 and 5 have many aspects pertaining to the distributions. The dark grey columns represent histograms of the underlying experimental data distributions. The green colors indicate full assessment distributions and the blue colors indicate simplified assessment distributions. The light colors are the best fits to the data, while the dark colors represent the conservative 95% lower bound distributions prescribed for computation in the Code. The dark blue solid vertical line is S_g and the dashed dark blue vertical line is $R_{tf} * S_g$. Note that S_g is found using the lower bound distribution for the simplified assessment. The solid dark green line is the stress at a $POF = 10^{-4}$ using the full assessment lower bound distribution, for reference.

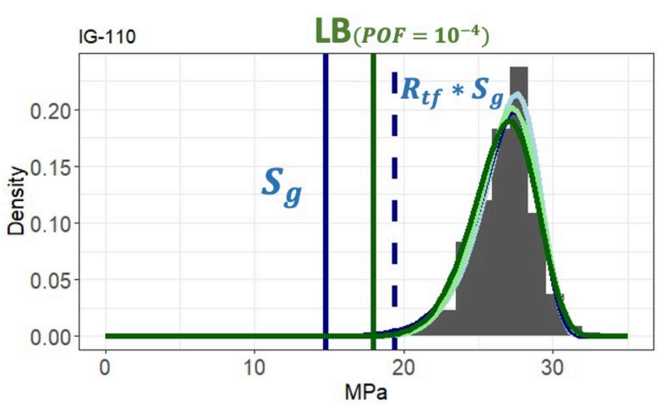

Figure 4: IG-110 DISTRIBUTIONS

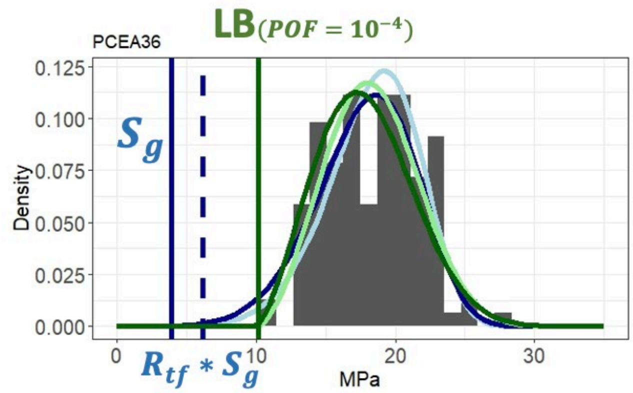

Figure 5: PCEA36 DISTRIBUTIONS

2.5.2 FE Model Component Stress Data

The finite element model for the tensile dog-bone specimen was created under the assumption of purely elastic behavior. Therefore, once a stress state has been determined in the analysis, the magnitudes for each stress can be scaled by the load of interest.

The values of tensile strength collected during the mechanical testing of these components correspond to the maximum engineering stress experienced in the small diameter section of the sample at the moment immediately prior to failure. The component stresses in the model can be scaled to match whatever strength value is of interest in the study.

For this analysis, fully integrated 8-noded elements were used. The integration point values for each element in the mesh were combined to a weighted element average for each principal stress value. For each element, the three principal stresses were combined in accordance with HHA-3213 to form an average equivalent stress for each element. It is worth noting that this may not be the process that is directly outlined in the ASME Code, which states that values are to be determined at each integration point, and the associated volume for that point is to be used in the grouping step.

Although the Code specifies that this procedure be done on integration points, it is common practice to use element volumes and element-averaged quantities. Development work is currently underway in Grizzly to implement the simplified and full assessments so that the FE model can directly output peak equivalent stress and POF values.

2.6 Dog-bone Analysis

Dog-bone geometries and graphite grades IG-110 and PCEA36 were used for comparison. The results are compared for FE applied to high and low loads in the full and simplified assessments. The low loads were found to straddle the 10^{-4} limit.

V_m and Δ criteria were changed between the 2019 and 2021 Code versions in the full assessment; therefore, both were considered. Table 2 provides the V_m and Δ criteria for both the 2019 and 2021 Code versions, for both grades. V_m was calculated using $K1c\ (\frac{MPa}{\sqrt{m}})$ values of 1.33 for PCEA36 and 1.07 for IG-110.

Table 2: VOLUME GROUPING CRITERIA FOR IG-110 AND PCEA

Grade/ Code Version	2019; $\Delta = 0.07$	2021; $\Delta = 0.2$
IG-110 V_m (mm^3)	0.008	14.704
PCEA V_m (mm^3)	512	572.104

The scope of this study contains comparisons according to Table 3.

Table 3: STUDY MATRIX

Target POF	IG-110		PCEA36	
High	2019	2021	2019	2021
Low	2019	2021	2019	2021

The fitted quantiles used to scale the FE applied load for PCEA36 and IG-110 are summarized in Table 4. For a realistic application of the Code, different applied pressure loadings would not be applied for the full and simplified assessments for a given component. Different applied pressure loadings were used for illustration purposes in the full and simplified assessments in this paper. As expected, target applied pressure loadings associated with the higher quantile are very similar when using the 2- and the 3-parameter Weibull distributions (simplified and full). However, the non-zero threshold parameter greatly shifts the target pressure loading to the right in the left tail of the distribution (near the target POF=10^{-4}).

Table 4: GRAPHITE GRADES AND APPLIED PRESSURE LOADINGS (MEMBRANE STRESS)

Low Target	Simplified (MPa)	Full (MPa)
IG-110	14.77	15.5
PCEA36	3.877	6.2
High Target		
IG-110	26.842	26.723
PCEA36	18.082	17.6734

3. RESULTS AND DISCUSSION

3.1 Results

3.1.1 Simplified Assessment

The dog-bone meshes showed slightly increasing peak equivalent stresses with increased mesh refinement because of elevated stresses at the fillet radius. Whether the changes in mesh refinement affect the acceptance decision is dependent on how close the applied stress in the FE model is to the allowable stress value. Table 5 provides $S_g(10^{-4})$ and the allowable stress value $[R_{tf} * S_g(10^{-4})]$ for both grades in MPa.

Table 5: SIMPLIFIED ASSESSMENT ACCEPTANCE METRICS FOR IG-110 AND PCEA36

Grade/Metric	$S_g(10^{-4})$ MPa	$R_{tf} * S_g(10^{-4})$ MPa
IG-110	14.77	19.386
PCEA36	3.877	6.188

Peak equivalent stresses are listed below in Tables 6 and 7 from each of the five dog-bone meshes for IG-110 and PCEA36 at the two target membrane stresses applied in this study. The high applied loads result in failure at the membrane stress check. The low applied load was set to the S_g limit, allowing passing of the membrane stress check. However, components failed the peak equivalent stress check, regardless of mesh refinement.

For IG-110, the relative change in peak equivalent stresses between each level of mesh refinement was <2%. Both applied stresses resulted in peak equivalent stresses above the $R_{tf} * S_g = 6.188\ MPa$ limit, therefore mesh refinement did not affect acceptance for these applied stresses. However, with peak equivalent stresses increasing by nearly 1 MPa between the least and most refined meshes, one could conceivably apply a stress in which mesh refinement could affect the results of the second check in the simplified assessment.

Table 6: PEAK EQUIVALENT STRESSES FOR IG-110

Membrane Stress/Mesh	1	2	3	4	5
14.77 MPa	14.812	14.866	15.194	15.411	15.493
18.082 MPa	18.133	18.199	18.601	18.867	18.968

The conclusions made in Table 6 for IG-110 are also applicable to the results for PCEA36 in Table 7.

Table 7: PEAK EQUIVALENT STRESSES FOR PCEA36

Membrane Stress/Mesh	1	2	3	4	5
3.877 MPa	3.888	3.901	3.986	4.042	4.063
18.082 MPa	18.134	18.196	18.589	18.851	18.950

3.1.2 Full Assessment

The full assessment is performed by comparing a component POF to the SRC POF limit. In general, the change in POF is minimal for the finest two meshes. This POF trend did not entirely hold for IG-110 when applying the 2019 Code rules. It is hypothesized that the small V_m is still causing enough changes in the POF to warrant further mesh refinement before saying the POF has converged. Figure 6 displays the lower pressure loading results. The black dashed lined is the

POF=10^{-4} limit. Results at the low pressure loadings show how mesh refinement can affect the acceptance decision.

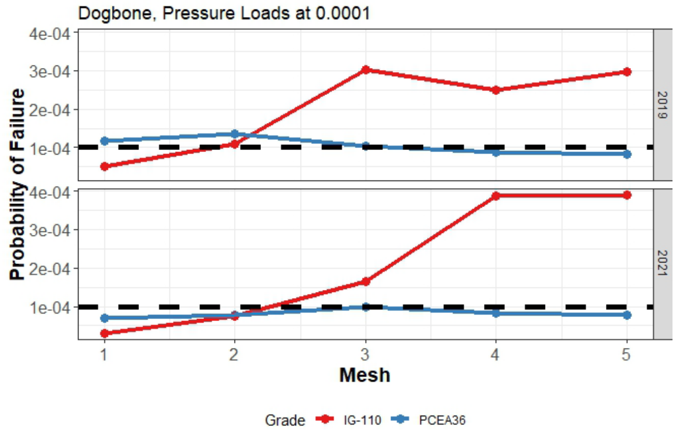

Figure 6: FULL ASSESSMENT RESULTS FOR THE EFFECTIVE 0.0001 APPLIED LOADINGS

Figure 7 displays the results at the higher pressure loadings. The loads were high enough to not affect the acceptance decision. However, the plot displays that POF convergence did not happen until the 3rd or 4th level of mesh refinement.

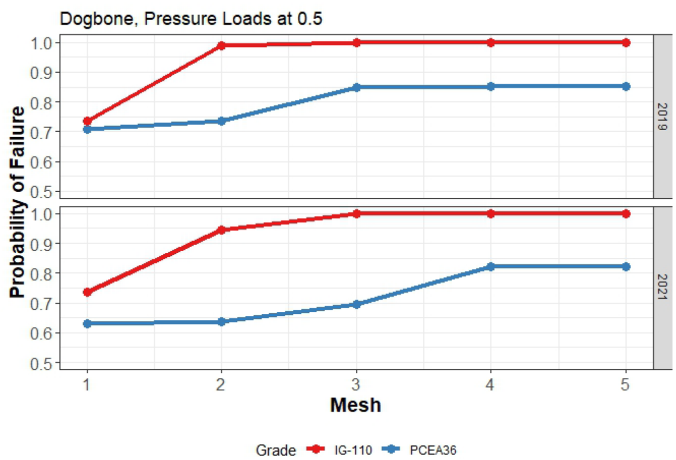

Figure 7: FULL ASSESSMENT RESULTS FOR THE EFFECTIVE 0.5 APPLIED LOADINGS

Figure 8 displays the fractional change in POF as a function of the fractional change in peak equivalent stress. Fractional change for arbitrary x relative to previous x0 is: $|\frac{x-x0}{x0}|$. The change in POF converges to less than one between meshes 4 and 5 for both pressure loadings.

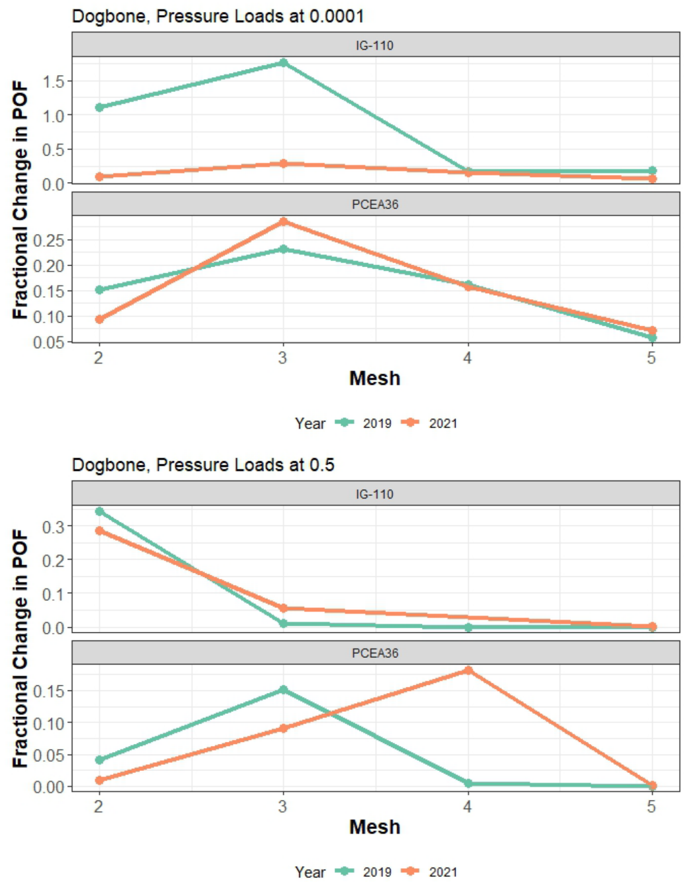

Figure 8: FRACTIONAL CHANGE IN POF AS A FUNCTION OF MESH

3.2 Discussion

This mesh convergence study showed slightly increasing peak stress values around the surface of the fillet region of the component with increased mesh refinement. This behavior is common in models where there are abrupt changes in the geometry, such as sharp corners, holes, fillets, and notches. The dog-bone geometry considered for analysis in this paper contains a fillet where the large cross-section is reduced to the smaller cross-section found in the center of the sample. This is commonly referred to as a stress riser or stress concentration, where the computed stresses in the FE model are elevated due to geometric factors. This can be problematic when considering the simplified assessment as only the peak equivalent stress is considered in the second check. In practice, only the neck portion of the dog-bone is important when applying the tensile test. The methods applied in this study used the entire dog-bone FE model, rather than sub-setting to the neck portion in order to illustrate how complex geometries may affect the mesh refinement necessary when applying the simplified and full assessments.

Stress concentrators may require more mesh refinement than is typical to get convergence in simplified assessment results. In such cases, where the peak stress is near the allowable stress value, it would be wise to consider using the full assessment for further investigation. However, if the peak stresses are far lower than the acceptable limits, it may not be necessary to further refine the mesh.

One may think the grouping of elements in the full assessment would mask any mesh refinement effects. Though not conclusive, this study suggests that the magnitude of V_m relative to the mesh element volumes influences the degree to which mesh refinement affects the POF. V_m is substantially smaller in the 2019 Code version for IG-110, and we see the POF continuing to rise with mesh refinement for the lower applied loadings (10^{-4}), whereas the POF appears to level off for Meshes 3-5 for all other cases. This suggests that the larger V_m values result in POFs that are less sensitive to the micro-changes in element stresses that come with continued mesh refinement. This effect only appeared with the lower pressure loading.

As mentioned, the current HHA-3000 Code sections do not provide guidelines for mesh refinement. However, that is not uncommon. For example, Subpart B on Composite Materials [3] utilizes a similar methodology as the simplified assessment for component acceptance and does not provide guidelines for mesh refinement. Depending on the geometry and the loading applied, stress convergence within a model may not equate to POF convergence within that same model. Additional mesh refinement studies are currently underway that evaluate these statements for other geometries and graphite grades.

Though this paper focused on the mesh refinement effects on acceptance decisions in the full and simplified assessments, other items of interest pertinent to the methodologies are illustrated in this study. Those include:

- When searching for a load that resulted in a POF=10^{-4} in the full assessment for PCEA36, initially the 10^{-4} load based on the 3-parameter lower bound distribution was used, around 10 MPa. This resulted in a POF ~0.007 for Mesh 3. However, in an experiment where the threshold was not reduced, the peak equivalent stress quickly became less than the original threshold parameter as the load of 10 MPa was reduced, in an attempt to achieve a load associated with a POF=10^{-4}. The peak equivalent stress less than the threshold results in a POF=0 when the threshold reduction step is removed. It is hypothesized that one reason for the threshold reduction step is to avoid situations like this, which absent the threshold reduction step would not have allowed the component to obtain a POF between 0 and ~0.007.
- In the full assessment, originally, applied stresses at the 10^{-4} target POF were found using the 3-parameter Weibull lower bound distribution. However, the resulting POF's were much larger than 10^{-4} (by at least one order of magnitude). The major reason for this is that the 3-parameter Weibull lower bound distribution is used at the beginning of the full assessment, however, after the threshold reduction step, a new 3-parameter Weibull distribution is used in the final POF calculations. Since this new distribution has a decreased threshold, that can greatly affect the amount area below the 10^{-4} quantile of the distribution relative to the original 3-parameter Weibull distribution. This is believed to work as intended in the full assessment. In addition to reasons for the threshold reduction identified in the first bullet, the threshold is reduced to account for the fact that enough data are not collected to characterize the left tail of the Weibull distribution well experimentally, and to add in conservatism since the Code does not prescribe using a lower bound on the threshold parameter.
- The "new" or reduced 3-parameter Weibull distribution changes slightly depending on the peak equivalent stress. Since mesh refinement affects peak equivalent stress, slightly different reduced Weibull distributions were used in the final POF calculation depending on mesh refinement. Though, when looking into this further, differences in reduced 3-parameter Weibull distributions were minimal in terms of parameters used.
- Finally, Figures 4 & 5 illustrate that the relationship between the simplified assessment limits and the stresses associated with the POF=10^{-4} in the 3-parameter Weibull lower bound distribution in the full assessment can change by graphite grade. These are not artifacts of the methodologies used in the assessments, but rather in the material properties as they present themselves in the Weibull fits to the experimental data.

4. CONCLUSION

This study set to determine mesh refinement effects on the acceptance decision of nuclear grade graphite core components per Article HHA-3000 of the ASME BPV Codes [3]. Five mesh refinement levels were considered, with the peak equivalent stress changing by less than 2% for the three finest meshes. Mesh refinement did not affect the simplified assessment acceptance decisions for the applied pressure loadings in this study. However, since the peak equivalent stresses changed by nearly 1 MPa between the least and most refined meshes, it is conceivable that a case exists where mesh refinement could affect the acceptance decision in the simplified assessment.

Mesh refinement affected the full assessment acceptance decisions for the low applied pressure loadings in this study for both grades, even though peak equivalent stresses changed by less than 2%. POF did not hit convergence until the 3rd or sometimes 4th mesh refinement. This suggests that FE modelers need to evaluate POF convergence as a criteria for sufficient mesh convergence running components through the full assessment. It is hypothesized that smaller minimum link volumes necessitate more extensive mesh refinements to achieve POF convergence due to sensitivities in micro-changes to mesh element stresses that appear during mesh refinement. This study suggests POF convergence appears to happen after stress distribution convergence, contrary to previous work done by Hindley in [4]. POF convergence needs to be considered when determining adequate FE stress distribution convergence, especially when the calculated component POF is near the SRC limit.

ACKNOWLEDGEMENTS

The authors would like to thank those that contributed to the Unirradiated Graphite Testing Baseline Program, for providing the necessary data, as well as the Design Task Group members for the shared knowledge and understanding of these assessments.

REFERENCES

[1] Benjamin W. Spencer, William M. Hoffman, Sudipta Biswas, Wen Jiang, Alain Giorla, and Marie A. Backman, (2021). "Grizzly and BlackBear: Structural component aging simulation codes," Nuclear Technology, 207:7, 981-1003, DOI: 10.1080/00295450.2020.1868278

[2] Cody J. Permann, Derek R. Gaston, David Andrš, Robert W. Carlsen, Fande Kong, Alexander D. Lindsay, Jason M. Miller, John W. Peterson, Andrew E. Slaughter, Roy H. Stogner, Richard C. Martineau, (2020). "MOOSE: Enabling massively parallel multiphysics simulation," SoftwareX, Volume 11, 100430, ISSN 2352-7110.

[3] American Society of Mechanical Engineers (ASME) Boiler and Pressure Vessel Code (BPVC), Section III, Rules for the Construction of Nuclear Facility Components, Division 5, High Temperature Reactors, (2011). New York.

[4] Michael P. Hindley, Mark N. Mitchell, Christiaan Erasmus, Ross McMurtry, Thorsten H. Becker, Deborah C. Blaine, and Albert A. Groenwold, (2013). "A numerical stress based approach for predicting failure in NBG-18 nuclear graphite components with verification problems," Journal of Nuclear Materials, 436(1-3): pp. 175-184. https://doi.org/10.1016/j.jnucmat.2012.10.030

[5] Josina W. Geringer, Timothy D. Burchell, Mark Mitchell, (2021). "ASME NTB: Background information for addressing adequacy or optimization of ASME BPVC Section III, Division 5 rules for nonmetallic core components."

[6] T. R. Allen, K. Sridharan, L. Tan, W. E. Windes, J. I. Cole, D. C. Crawford, Gary S. Was, (June 2008). "Materials challenges for Generation IV nuclear energy systems," Nuclear Technology, Vol. 162(3), pp. 342-357.

[7] B.J. Marsden, A.N. Jones, G.N. Hall, M. Treifi, P.M. Mummery, "Graphite as a core material for generation IV nuclear reactors," in: Structural Materials for Generation IV Nuclear Reactors, Elsevier, 2017, pp. 495–532, https://doi.org/10.1016/B978-0-08-100906-2.00014-8.

[8] J. Kane, C. Karthik, D. P. Butt, W. Windes, and R. Ubic, (2011). "Microstructural characterization and pore structure analysis of nuclear graphite," Journal of Nuclear Materials, 415 (2) 189-197. https://doi.org/10.1016/j.jnucmat.2011.05.053

[9] C. Karthik, J. Kane, D. P. Butt, W. Windes, and R. Ubic, (2012). "Microstructural characterization of next-generation nuclear graphites." Microscopy and Microanalysis, 18(2) pp. 272-278.

[10] D. Kanse, I.A. Khan, V. Bhasin, R.K. Singh, (2015). "Interpretation of ASME Code rules for assessment of graphite components". SMiRT23, Division II, Paper ID 346.